Hindawi
International Journal of Antennas and Propagation
Volume 2019, Article ID 4732905, 7 pages
https://doi.org/10.1155/2019/4732905

Research Article

A Compact Dual-Band CPW-Fed MIMO Antenna for Indoor Applications

Mohamed M. Morsy

Electrical Engineering Department, Texas A&M University-Texarkana, Texarkana, TX 75503, USA

Correspondence should be addressed to Mohamed M. Morsy; mmorsy@tamut.edu

Received 10 December 2018; Accepted 23 February 2019; Published 17 April 2019

Academic Editor: Miguel Ferrando Bataller

A compact dual-band multiple-input-multiple-output (MIMO) antenna for LTE700, GSM1900, and UMTS applications with high isolation is presented. To enhance impedance matching and multiband operation, two inverted L-shaped monopoles are printed in the circular slot of the ground plane. The single element design is mirrored along the diameter of the circular slot of the ground plane. A strip is employed between the two radiators in order to mitigate the mutual coupling effect and enhance the impedance matching at operating bandwidths. Moreover, two slits are inserted in the ground plane in order to disturb the current distribution between radiating elements, and hence, the isolation between elements is improved. The measured 10 dB return loss bandwidth is 100 MHz (698–798 MHz) and 359 MHz (1765-2124 MHz) over the LTE700, GSM1900, and UMTS bands. The measured isolation between the two ports is less than -13 dB over the LTE700 bands while it is recorded to be less than -17 dB over the GSM1900 and UMTS bands. In addition, parametric studies of the proposed MIMO antenna are performed, and the surface current analysis is discussed to show the effect of the isolation structure. The radiation patterns are measured, and envelope correlation coefficient is calculated. The simulated results are in good agreement with measurements.

1. Introduction

With the fast development of the industry of wireless communication, there is an increase in the demand of multiband and highly isolated MIMO antennas for terminal users of cellular networks and indoor base stations. In 2018, it is estimated that cellular networks cover almost 95% of the global population, while LTE currently covers over 60% of the world's population and is expected to grow to more than 85% in 2023 [1]. While there is uncertainty about 5G deployment, it has been confirmed that 5G deployment will partially rely on existing LTE networks that could be easily updated to support 5G coverage using existing LTE bands [2]. MIMO antennas can support data reliability and increase the channel capacity while using several antennas at both transmitting and receiving terminals. A common application of MIMO antennas is for WLAN, LTE, GSM, and UMTS coverage. Lately, there has been an increase in the demand of indoor base stations/repeaters for indoor small coverage [3–7]. In [3], the proposed antenna covers a broadband bandwidth (1710-2690 MHz); however, the wide bandwidth is achieved by employing a complex structure of parasitic elements and a cavity of electric wall that raises the question about the feasibility of implementation in user's terminals or compact indoor base stations. In [4], a nonplanar dual-band antenna with large ground plane is presented. In [5], a Vivaldi antenna is used to achieve the LTE band 4 (1.7-2.1) GHz. Coplanar waveguide (CPW) microstrip antennas have also proven to be good candidates for MIMO applications [8]. The dual-polarized CPW MIMO antenna in [8] operates at 5.0 GHz and provides a high isolation. The literature of recently published single-element CPW planar microstrip antennas has shown a strong potential for employing planar CPW in MIMO designs [9–11].

Based on the aforementioned literature, we propose a novel design of CPW-fed MIMO antenna for GSM/UMTS/LTE system. The radiating elements consist of two parallel inverted L-shaped conductors at two opposite ends of the antenna's substrate. By inserting the radiators into the circular ground slot while separating both radiators by employing a parasitic strip between them, a good impedance matching and high isolation are achieved. To further enhance isolation

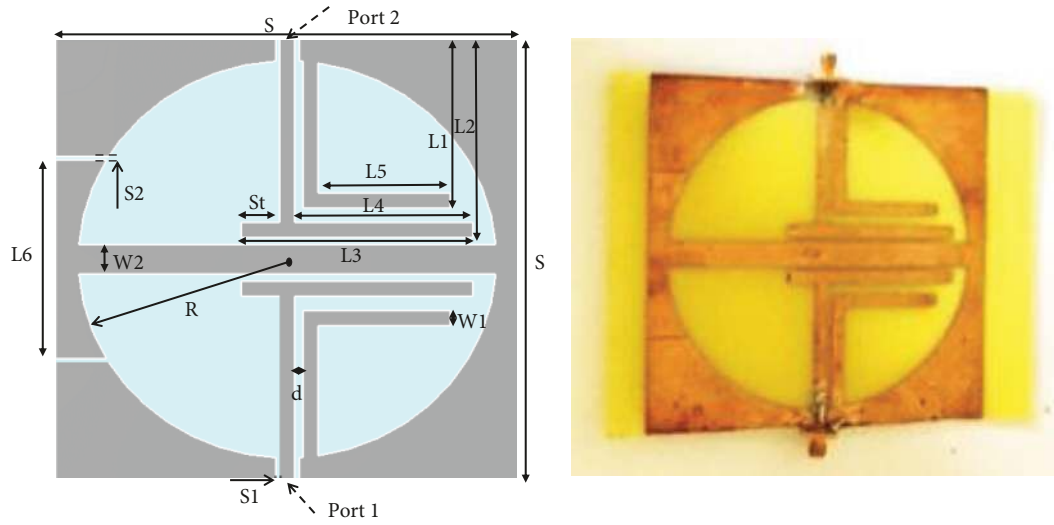

Figure 1: (a) Geometry of the proposed antenna; (b) photograph of the fabricated antenna.

Table 1: Details of antenna parameters (all dimensions are in mm).

S	120	**L5**	34	**S2**	0.4
L1	46	**L6**	54	**St**	10
L2	54	**W1**	4	**d**	2
L3	60	**W2**	8	**R**	54
L4	46	**S1**	0.4		

between MIMO elements, two slits are inserted in the ground conductor. The measured 10 dB return loss is 100 MHz (698–798 MHz) and 359 MHz (1765-2124 MHz) over the LTE700 and GSM1900/UMTS bands, respectively. The measured isolation between the two ports is higher than 13 dB over the LTE700 bands while it is recorded to be higher than 17 dB over the GSM1900 and UMTS bands.

2. MIMO Antenna Configuration

The geometry of the proposed MIMO antenna is shown in Figure 1(a). It is fabricated on a 0.8 mm FR4 epoxy substrate with permittivity $\varepsilon_r = 4.4$ and loss tangent $\tan\delta = 0.02$. The antenna consists of two symmetrical radiating elements that are inserted into the circular ground slot of radius, R. Each element consists of two parallel L-shaped conductors. The coplanar waveguide (CPW) conductors of 50 Ω are used to feed the radiating elements. There is a horizontal strip with a width of W2 that is used to mitigate the mutual coupling effect between the symmetrical elements. All radiating L-shaped strips and CPW feedlines are of width, W1. Two slits of width, S1, are etched on the left side of the ground plane in order to disturb the current distribution between radiating elements and thus improve isolation between radiating elements. The antenna geometrical parameters are given in Table 1. Figure 1(b) shows a photograph of the fabricated antenna.

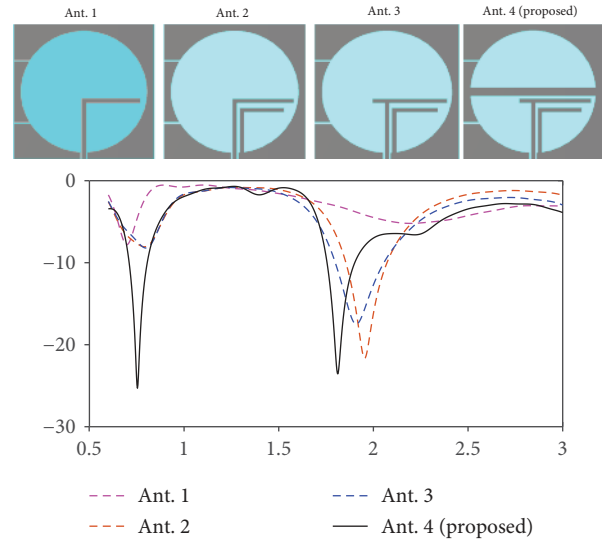

Figure 2: Simulated return loss of different designs.

The design process of each element consists of four main phases evolving from antenna 1 to antenna 4 as depicted in Figure 2. Antenna 1 is a classic coplanar waveguide (CPW) formed by an L-shaped conductor separated from a pair of ground planes, and all are on the same plane. It is seen that antenna 1 generates two resonances over the UMTS (1.7-2.2 GHz) and LTE700 bands. However, the resonance modes of the UMTS and LTE700 bands do not show good impedance matching for both bands. In antenna 2, a parallel L-shaped strip is inserted on the right of the L-shaped CPW line. It is seen that the impedance matching has significantly improved over the UMTS band; however, the LTE700 band still exhibits poor matching. A slight improvement of widening the bandwidth of the UMTS band is achieved by adding a matching stub, St, as shown in antenna 3. In antenna 4, a

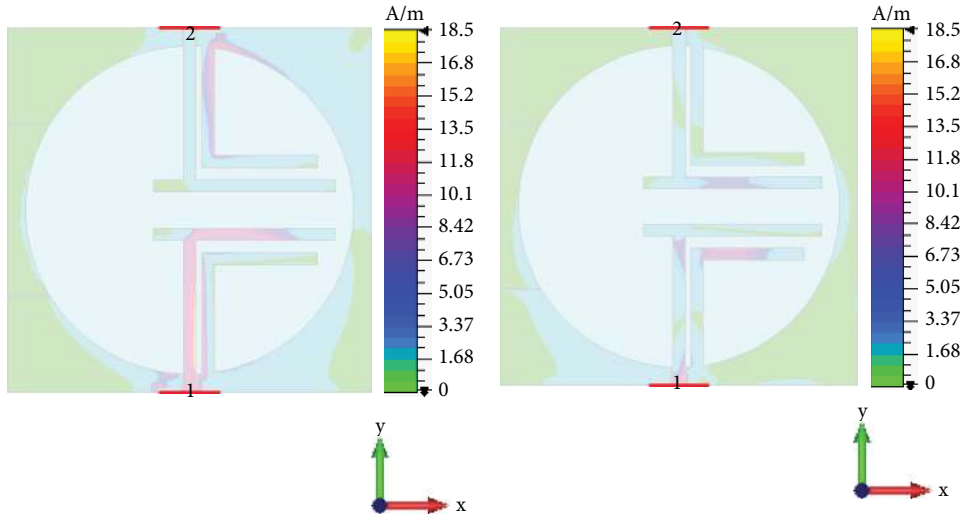

Figure 3: Current distribution of the proposed antenna without the isolation structure (a) at 0.75 GHz and (b) at 1.9 GHz.

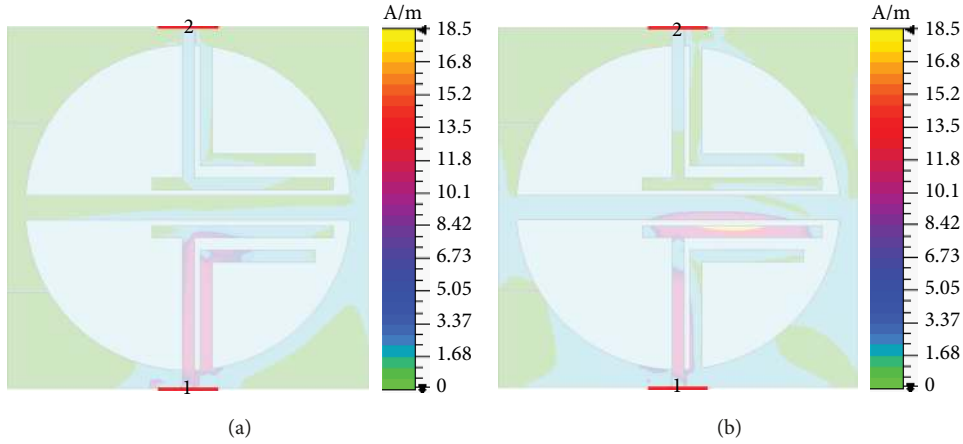

Figure 4: Current distribution of the proposed antenna with the isolation structure (a) at 0.75 GHz and (b) at 1.9 GHz.

conducting strip is used to connect both sides of the ground plane. It can be seen that this antenna has good impedance characteristics over both the LTE700 and UMTS bands. Next, the two L-shaped strips of antenna 4 are mirrored to form the proposed 2 × 2 MIMO antenna system as shown in Figure 1.

In order to gain more insight into the isolation behaviour of the proposed MIMO antenna, Figures 3 and 4 present a comparison of the current distributions of the proposed design without and with the isolation structure, respectively. Figure 4 shows the surface current distribution (A/m) of the proposed MIMO antenna without the center metal strip that acts as the isolation structure between the radiating elements. The surface current is simulated by exciting one input (port 1) of the two-element MIMO antenna system, while terminating the other element (port 2) to a 50 Ω load. It is noticed that a large amount of surface current flows from port 1 to port 2 at 0.75 GHz and 1.9 GHz as shown in Figures 3(a) and 3(b), respectively. After employing the isolation structure, the current paths are disturbed by the isolation structure at 0.75 and 1.9 GHz, as shown in Figures 4(a) and 4(b), respectively. In fact, the center strip connecting the two sides of the ground plane acts as a resonator that disturbs the current paths from port 1 to port 2 at operating frequencies and hence improves isolation between MIMO elements.

3. Experimental Results and Discussion

Due to the symmetry of radiating elements, most measurement has been performed on port 1 of the proposed MIMO antenna while terminating port 2 with a 50 Ω load. The s-parameters of the proposed antenna are measured using the vector network analyser. Figure 5 shows the simulation and measured results of $|S_{11}|$. The measured 10 dB $|S_{11}|$ shows that the proposed MIMO antenna covers the LTE700, GSM1900, and UMTS bands. As illustrated in Figure 3, the isolation is dramatically improved with the use of the center strip connecting both sides of the ground plane, and the insertion of two slits on the left side of the ground plane. Figure 6 shows the measured and simulated $|S_{21}|$ of the proposed MIMO antenna with the isolation structure. The measured isolation $|S_{21}|$ is less than -13 dB and -17 dB over the LTE700 and UMTS bands, respectively.

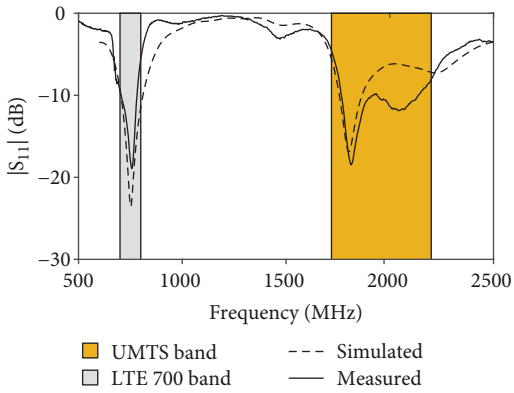

Figure 5: Measured and simulated $|S_{11}|$ of the proposed MIMO antenna.

Because it is not feasible to measure a 3D pattern, a multiple number of 2D polar patterns are measured. By aggregating these pattern cuts, a good approximation of the 3D pattern is obtained and the maximum gain is determined. By using the spherical coordinate systems, these 2D polar patterns are obtained by varying θ while fixing ϕ (elevation pattern) or fixing θ and varying ϕ (azimuth pattern). In order to measure different 2D pattern cuts, the mounting structure of the measuring system rotates in various planes by varying θ and ϕ. The peak gain of the proposed MIMO antenna is plotted in Figure 7. Although the antenna shows a relatively low gain at the 700 MHz band, the antenna remains suitable for indoor applications that do not rely on batteries for power such as routers and repeaters. The low gain in the 700 MHz band is attributed to the CPW feeding method that does not provide sufficient ground size and the use of isolation structure in conjunction with the ground plane. The radiation patterns of the proposed MIMO antenna were measured in the xy, xz, and yz planes at 0.75 GHz and 1.9 GHz as shown in Figure 8. The measurements were performed by exciting port 1 while terminating port 2 with a 50 Ω load. The measured and simulated radiation patterns are generally in good agreement with insignificant differences at some angles due to inaccuracy of the fabrication of the prototype. It is seen that the MIMO antenna system shows omnidirectional patterns in three orthogonal planes.

Envelope correlation coefficient (ECC) is crucial in evaluating the diversity performance of MIMO systems.

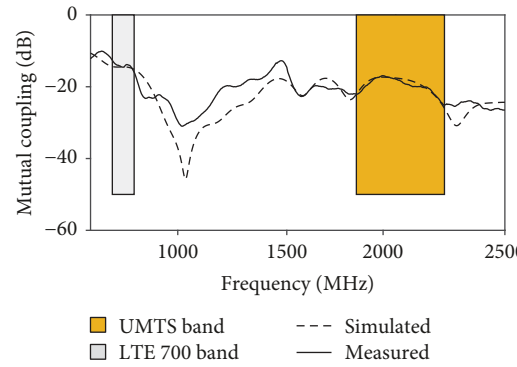

Figure 6: Measured and simulated $|S_{21}|$ of the proposed MIMO antenna.

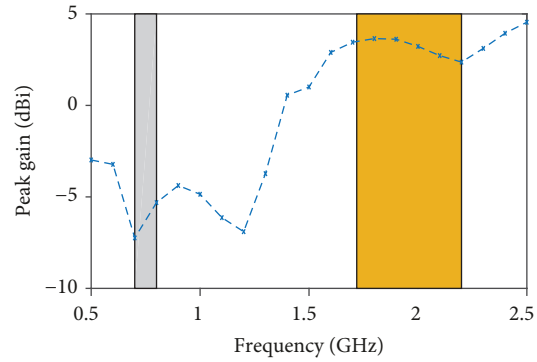

Figure 7: Peak gain of the proposed MIMO antenna.

Typically, an ECC < 0.5 is considered acceptable for mobile communications [12]. ECC can be evaluated from s-parameters as shown in [13].

$$\rho_e = \frac{\left|S_{11}^* S_{12} + S_{21}^* S_{22}\right|^2}{\left(1 - \left(|S_{11}|^2 + |S_{21}|^2\right)\right)\left(\left(1 - \left(|S_{22}|^2 + |S_{12}|^2\right)\right)\right.}. \quad (1)$$

However, calculating ECC from s-parameters is proven to be inaccurate for low-efficiency MIMO systems [14]. Alternatively, the far-field patterns provide a reliable measure of ECC for MIMO systems [15]. An approximation formula for ECC calculation using far-field patterns is given as

$$\begin{aligned}
\rho_e &= \frac{A}{B1B1},\\
A &= \oint\{\text{XPR}.\, E_{\theta 1}(\Omega)E_{\theta 2}^*(\Omega)P_\theta(\Omega) + E_{\varnothing 1}(\Omega)E_{\varnothing 2}^*(\Omega)P_\varnothing(\Omega)\}d\Omega,\\
B_1 &= \sqrt{\oint\{\text{XPR}.\, E_{\theta 1}(\Omega)E_{\theta 1}^*(\Omega)P_\theta(\Omega) + E_{\varnothing 1}(\Omega)E_{\varnothing 1}^*(\Omega)P_\varnothing(\Omega)\}d\Omega},\\
B2 &= \sqrt{\oint\{\text{XPR}.\, E_{\theta 2}(\Omega)E_{02}^*(\Omega)P_\theta(\Omega) + E_{\varnothing 2}(\Omega)E_{\varnothing 2}^*(\Omega)P_\varnothing(\Omega)\}d\Omega},
\end{aligned} \quad (2)$$

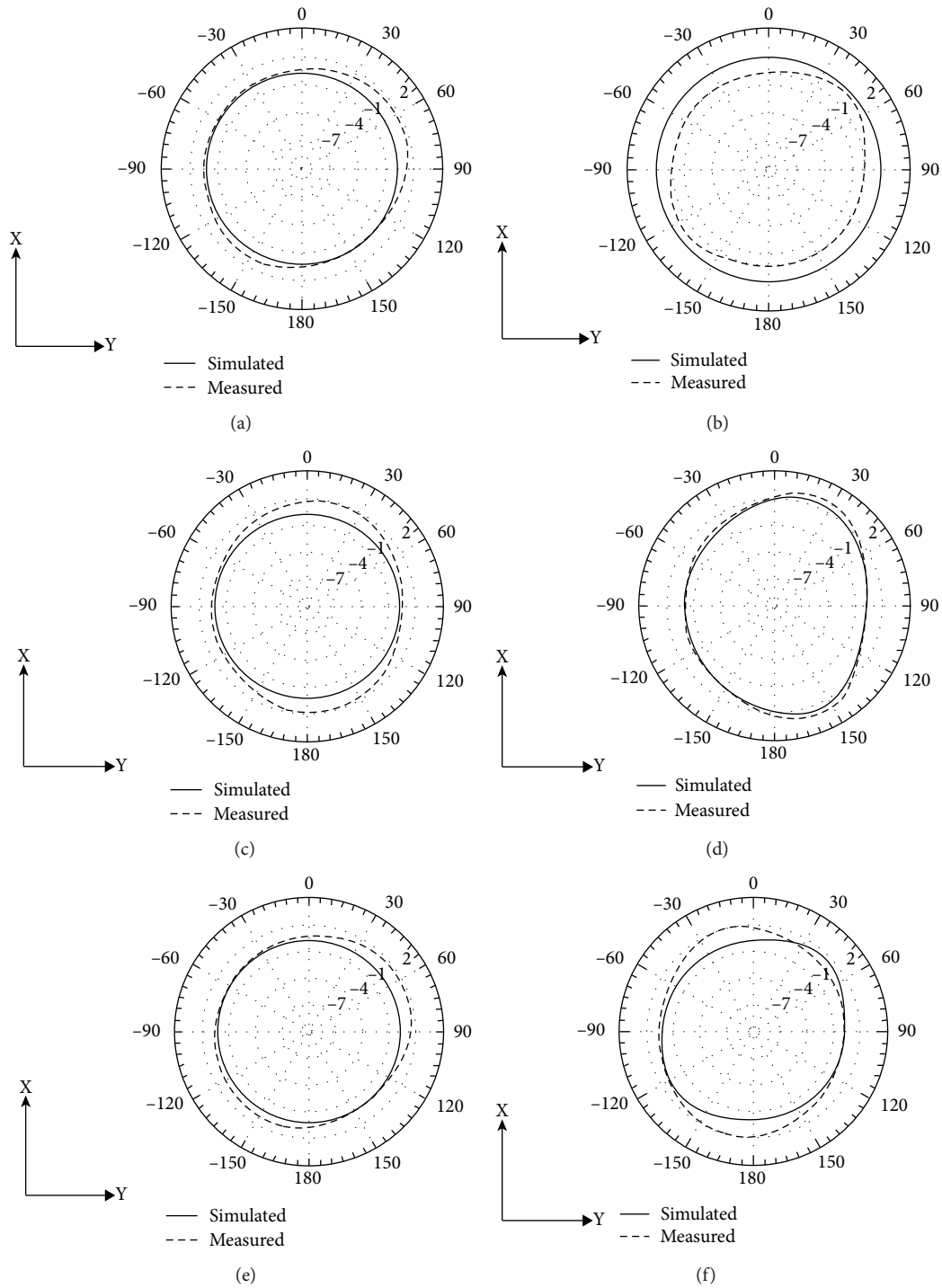

Figure 8: Directivity radiation patterns using linear scaling (a) XY plane at 0.75 GHz, (b) XY plane at 1.9 GHz, (c) XZ plane at 0.75 GHz, (d) XZ plane at 1.9 GHz, (e) YZ plane at 0.75 GHz, and (f) YZ plane at 1.9 GHz.

where XPR is the cross-polarization ratio, and $E_\theta(\Omega)$ and $E_\varnothing(\Omega)$ are the polarized θ- and ϕ-components of the antenna patterns, respectively. $P_\theta(\Omega)$ and $P_\varnothing(\Omega)$ are the θ- and ϕ -components of the angular power density functions of the incident plane wave, respectively, and Ω is the solid angle. In this paper, ECC is evaluated using both s-parameters and far-field pattern methods as shown in Figure 9. The ECC is below 0.02 over the operating bands when calculated from the s-parameters, while it is recorded to be less than 0.13 when calculated using the far-field radiation pattern.

The mean effective gain (MEG) and MEG ratio are considered important measures of diversity performance of MIMO antennas in wireless channels. MEG is the proportion of the received power to the incident power of the MIMO

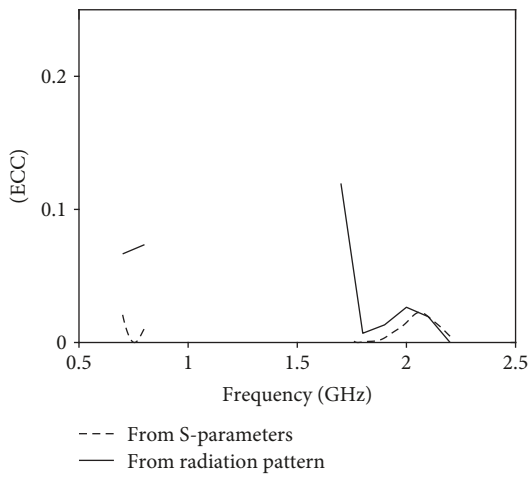

Figure 9: Calculated ECC using s-parameters and far-field patterns.

element. MEG takes into consideration the channel environment, polarization, and antenna's efficiency. It is expressed in the following equation [16]:

$$\mathrm{MEG} = \int \left(\frac{\mathrm{XPR}}{1+\mathrm{XPR}} G_\theta(\Omega) P_\theta(\Omega) + \frac{\mathrm{XPR}}{1+\mathrm{XPR}} G_\varnothing(\Omega) P_\varnothing(\Omega) \right) d\Omega. \quad (3)$$

For an isotropic environment, XPR = 0 dB and $P_\theta(\Omega) = P_\varnothing(\Omega) = 1/4\pi$. To achieve a good diversity performance, the ratio of MEG_1 and MEG_2 should satisfy the following criteria [12]:

$$\frac{\mathrm{MEG}_1}{\mathrm{MEG}_2} \cong 1, \quad (4)$$

where MEG_1 and MEG_2 are the MEGs of elements 1 and 2, respectively. The measured ECC and MEG ratio in the operating bands satisfy the diversity performance criteria for mobile communications; therefore, the proposed antenna is suitable for MIMO systems.

4. Conclusion

A low-profile CPW-printed MIMO antenna for indoor application is presented. The proposed antenna is based on employing two-inverted L-shaped conductors to radiate as a single element. The single element is mirrored around the diameter of the circular slot of the ground plane. A conductor strip is employed between the two elements in order to improve isolation and to further enhance the impedance matching at operating bands. Measured results show isolation that is less than -13 dB over the LTE700 bands while it is found to be less than -17 dB over the GSM1900 and UMTS frequency bands. Simulations and measurements are in good agreement for the LTE700, UMTS, and GSM1800/1900 bands. The measured results, including return loss, isolation, and radiation patterns as well as ECC, and MEG values, have shown that the proposed antenna system is a good candidate for MIMO applications with excellent isolation and diversity performance.

Data Availability

The data produced under this research will be available for sharing upon reasonable request to the author while safeguarding the intellectual property rights of the author.

Conflicts of Interest

The author declares that there is no conflict of interest regarding the publication of this paper.

References

[1] Ericsson, *Ericsson Mobility Report*, Ericsson, Stockholm, 2018, November 2018, from https://www.ericsson.com/assets/local/mobility-report/documents/2018/ericsson-mobility-report-june-2018.pdf.

[2] A. Haidine and S. E. Hassani, "LTE-a pro (4.5G) as pre-phase for 5G deployment: closing the gap between technical requirements and network performance," in *2016 International Conference on Advanced Communication Systems and Information Security (ACOSIS)*, pp. 1–7, Marrakesh, October 2016.

[3] H. Lee and B. Lee, "Compact broadband dual-polarized antenna for indoor MIMO wireless communication systems," *IEEE Transactions on Antennas and Propagation*, vol. 64, no. 2, pp. 766–770, 2016.

[4] Y. Zhao, "Dual-wideband microstrip antenna for LTE indoor base stations," *Electronics Letters*, vol. 52, no. 8, pp. 576–578, 2016.

[5] A. K. Arya, N. V. Anh, R. S. Aziz, B. Y. Park, and S.-O. Park, "Dual polarized dual antennas for 1.7–2.1 GHz LTE base stations," *IEEE Antennas and Wireless Propagation Letters*, vol. 14, pp. 1427–1430, 2015.

[6] Y. Yang, Q. Chu, and C. Mao, "Multiband MIMO antenna for GSM, DCS, and LTE indoor applications," *IEEE Antennas and Wireless Propagation Letters*, vol. 15, pp. 1573–1576, 2016.

[7] O. Soykin, A. Kolobov, V. Ssorin, A. Artemenko, and R. Maslennikov, "Planar MIMO antenna system with polarization diversity for 2.5–2.7 GHz LTE indoor FemtoCells," in *2015 9th European Conference on Antennas and Propagation (EuCAP)*, pp. 1–5, Lisbon, 2015.

[8] W. Li, Z. Zeng, B. You, L. Ye, Y. Liu, and Q. H. Liu, "Compact dual-polarized printed slot antenna," *IEEE Antennas and Wireless Propagation Letters*, vol. 16, pp. 1–2819, 2017.

[9] R. K. Saini, S. Dwari, and M. K. Mandal, "CPW-fed dual-band dual-sense circularly polarized monopole antenna," *IEEE Antennas and Wireless Propagation Letters*, vol. 16, pp. 2497–2500, 2017.

[10] M. O. Sallam, S. M. Kandil, V. Volski, G. A. E. Vandenbosch, and E. A. Soliman, "Wideband CPW-fed flexible bow-tie slot antenna for WLAN/WiMax systems," *IEEE Transactions on Antennas and Propagation*, vol. 65, no. 8, pp. 4274–4277, 2017.

[11] R. Cao and S.-C. Yu, "Wideband compact CPW-fed circularly polarized antenna for universal UHF RFID reader," *IEEE Transactions on Antennas and Propagation*, vol. 63, no. 9, pp. 4148–4151, 2015.

[12] R. G. Vaughan and J. B. Andersen, "Antenna diversity in mobile communications," *IEEE Transactions on Vehicular Technology*, vol. 36, no. 4, pp. 149–172, 1987.

[13] S. Blanch, J. Romeu, and I. Corbella, "Exact representation of antenna system diversity performance from input parameter description," *Electronics Letters*, vol. 39, no. 9, p. 705, 2003.

[14] P. Hallbjorner, "The significance of radiation efficiencies when using S-parameters to calculate the received signal correlation from two antennas," *IEEE Antennas and Wireless Propagation Letters*, vol. 4, pp. 97–99, 2005.

[15] S. Stein, "On cross coupling in multiple-beam antennas," *IRE Transactions on Antennas and Propagation*, vol. 10, no. 5, pp. 548–557, 1962.

[16] T. Taga, "Analysis for mean effective gain of mobile antennas in land mobile radio environments," *IEEE Transactions on Vehicular Technology*, vol. 39, no. 2, pp. 117–131, 1990.